Resource Potentials

*34 Brisbane Street, WA 6000*
*PO Box 167 Northbridge, WA 6865*
*Ph: (08) 9289 9100*
*Email: info@respot.com.au*
*Web: www.respot.com.au*

# Induced Polarisation surveying at the Ngalia Basin Project, Northern Territory, Australia

**For**

## ENERGY METALS LTD

Date: 27 November 2017

Authors: Aurore Joly, Nigel Cantwell, Matt Owers and Jayson Meyers
Resource Potentials Pty Ltd

Distribution: Wayne Taylor and Daniel Jordan
Energy Metals Ltd

# CONTENTS

Page

# 1. Introduction

Resource Potentials (ResPot) were commissioned to assist Energy Metals (EME) with IP survey planning, budgeting and contracting, survey monitoring and data QC, and then final data processing and imaging of IP survey data acquired at the Ngalia Basin Project in the NT during 2017. Detailed interpretation and targetting is excluded from the scope of work at this stage. New IP survey data acquired consisted of gradient array induced polarisation (GAIP) survey grids over the Dingo's Rest and Walbiri prospects and one pole-dipole IP (PDIP) traverse at the Yuendumu West prospect area (Figures 1 and 2).

The IP survey data were acquired by Zonge Australia during the period from the 31st of August to the 8th of September 2017 (see Zonge report by Mann, 2017). IP surveying was primarily carried out to identify reduced Mt Eclipse Formation sandstones containing pyrite, which are underlying transported and regolith cover sediments in this area, and have potential to contain uranium mineralisation. This approach was previously proven to be useful for interpretation and targetting following IP surveying carried out at the project in 2013. A total of 28 GAIP grids were acquired at the Ngalia Basin Project during 2013, including one survey grid at Dingo's Rest, and one survey grid at Walbiri (see Zonge report by Khrapov, 2013). No IP surveying has previously been carried out at the Yuendumu West prospect area prior to the recent PDIP surveying.

The 2013 Walbiri GAIP survey grid was positioned on the northern limb of an interpreted anticline, and a relatively high amplitude chargeability anomaly was observed in the gridded GAIP data, which appears to be associated with a reduced sandstone unit (Kerr and Taylor, 2015). The 2017 Walbiri GAIP survey grid was carried out on the interpreted southern limb of the anticline, to the southwest of the 2013 survey grid, in order to determine if a reduced sandstone unit was present on the southern limb.

The 2013 Dingo's Rest GAIP survey grid was positioned on a northwest bend within the Yuendumu thrust splay system (Figure 1; Kerr and Taylor, 2015). Relatively strong and broad IP chargeability anomalism is observed in the gridded GAIP data (shown later in Figure 5) and was interpreted as a reduced sandstone horizon, but the sandstone unit thickness was unknown due to lack of outcrop, and the width of the IP chargeability anomaly was considered to be likely due to a shallow dipping source layer with a reasonable depth extent. The strong chargeability anomalism was tested by multiple drill holes, but the results were disappointing, with no significant U mineralisation intercepted (Xiao et al., 2015). The 2017 GAIP survey grid was located to the south of the 2013 GAIP survey grid in order to map the extension of the Yuendumu thrust splay fault and possible reduced sandstones of the Mt Eclipse Formation. Historical trenches located in between the 2013 and 2017 GAIP survey grids, and encountering carnotite and high-grade mineralisation, enhance the prospectivity of this survey area.

The 2017 Yuendumu West PDIP traverse was oriented N-S across the major Yuendumu thrust in order to detect anomalous IP responses associated with the main thrust, and potential back thrusts that are interpreted by EME from airborne magnetic survey data previously acquired at the project in 2014 and processed by ResPot (Owers, 2015).

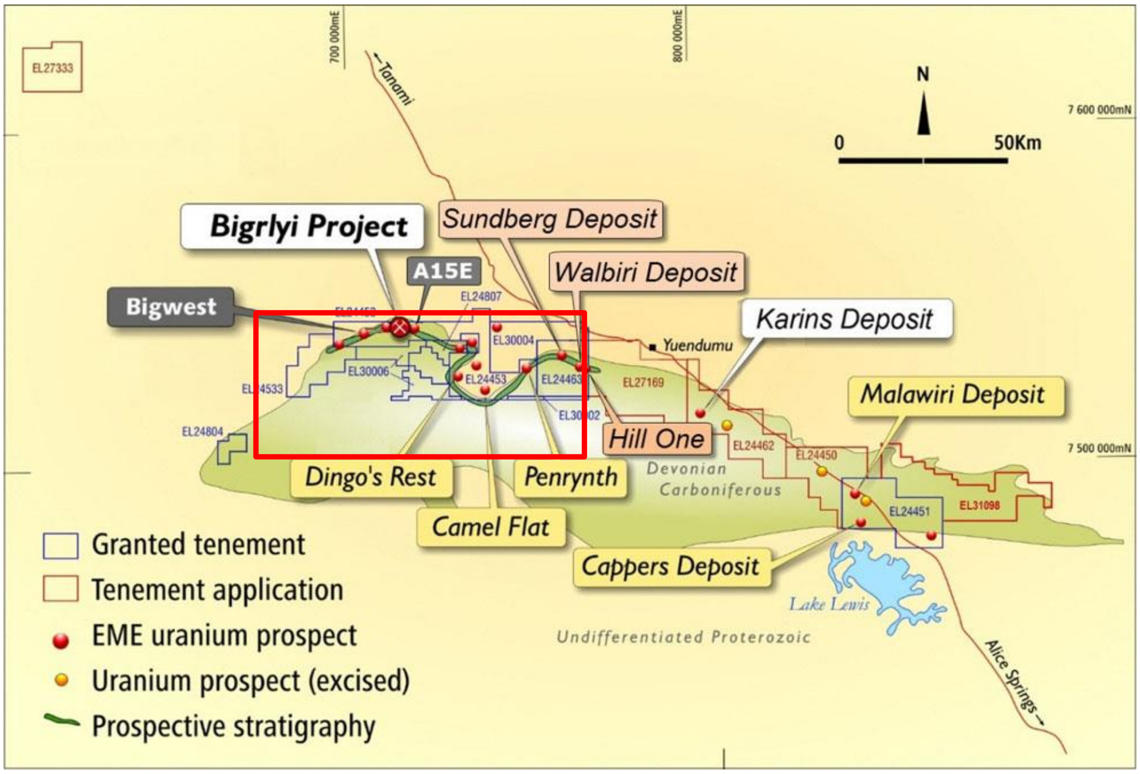


***Figure 1.*** *Regional scale map of uranium deposits and prospects, and EME exploration tenements within the Ngalia Basin Project. The red outline shows the map area displayed in Figure 2 (from Kerr and Taylor, 2015; Xiao et al., 2015).*

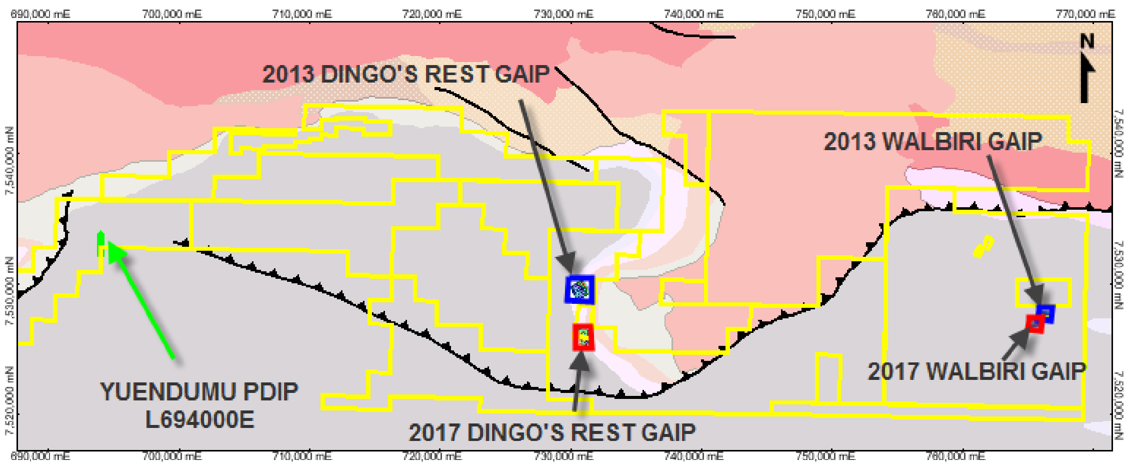


***Figure 2.*** *Ngalia Basin Project area tenements (yellow outlines) overlain on a simplified regional bedrock geology map. The Palaeozoic sedimentary rocks of the Ngalia Basin are shaded grey in the southern part of the map area, and the sedimentary rocks of the Paleoproterozoic Aileron Province are shaded pink in the northern part of the map area. The Yuendumu West PDIP survey line is shown by the green line in the western part of the map area. Both 2013 and 2017 GAIP survey grids are displayed as blue and red outlines.*

## 2. Induced Polarisation Background, Survey Data QC, Processing and Imaging

IP is an electrical geophysical survey method whereby positive and negative charged transmitter electrodes inject a galvanic electrical current into the ground, which causes electrons and ions to flow within the subsurface between these electrodes whilst the transmitter is turned on. Under these conditions, certain minerals will become polarisable along their grain boundaries, such as metallic sulphides, clays, graphite and some metal oxides. These chargeable minerals will hold an electrical charge, as clouds of polarised ions surrounding the surface area of minerals, for a discrete amount of time after the transmitter current is turned off. The return of the polarised ions to their natural state, and the decay of this electrical charge after the transmitter current is switched off (e.g. Figure 3), can be measured as a change in voltage over time between two receiver electrodes (a receiver dipole).

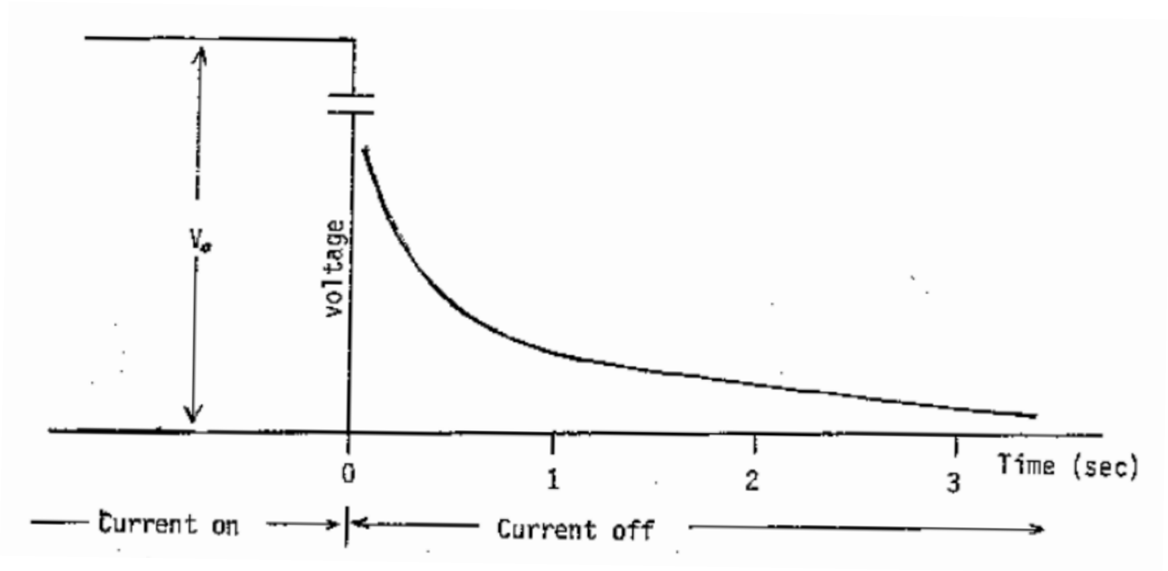


***Figure 3.*** *Typical IP decay curve showing how the voltage measured between two receiver electrodes decays after the transmitter current has been switched off.*

Measurements of apparent resistivity and chargeability are derived from the measurements of voltage between the field receiver electrode pairs. Resistivity is essentially a measurement of materials resistance to electrical current flow and is made from the primary voltage (measured voltage directly after the transmitter current is switched off). A greater current flow indicates less resistance and greater conductivity and, conversely, low current flow indicates greater resistance and lower conductivity. Resistivity responses measured in IP surveys are not typically directly related to the amount sulphide mineralisation, but may be observed over sulphide mineralised zones when there is disseminated sulphide mineral grains having a high total surface area, even if there is some degree of associated silicification, alteration and/or fracturing and faulting.

Chargeability reflects the ability to store an electrical charge over a specified time interval after the transmitter current has been switched off, and is calculated by integrating the IP decay cure (calculating the area beneath the decay curve) between a specified start and end time during the off-time period. A more chargeable source has a slower rate of decay of electrical charge, and therefore results in a greater area beneath the IP decay cure, which in-turn results in a greater calculated chargeability value.

The receiver dipoles are moved around within the survey area to take measurements. Transmitter and receiver electrodes can be arranged in a number of different survey array configurations. For the recent Ngalia Basin IP surveys, both the GAIP and PDIP survey configurations were used.

## 2.1. Gradient Array IP (GAIP)

### *2.1.1. Survey specifications, data QC and processing*

GAIP surveys are the simplest form of IP surveying, whereby the transmitter (Tx) current electrodes are placed outside of a small survey grid area (usually 1 x 1 km) and are oriented perpendicular to geological strike. The survey stations are then acquired along survey lines within the grid area using a dipole electrode receiver (Rx) pair along survey lines. The Rx reading location is corrected for its position relative to the Tx locations in order to normalise the IP readings across the survey grid, and is taken as the mid-point location of the Rx electrode pair. Figure 4 shows a typical GAIP configuration along a survey line.

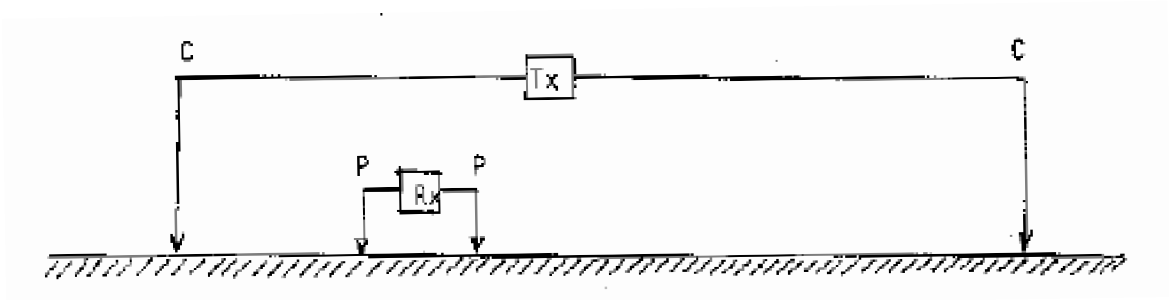


***Figure 4:*** *Schematic diagram of a GAIP survey configuration in an across line section view. The transmitter (Tx) current electrodes are placed outside of the survey grid area. The receiver (Rx) electrodes measure the voltage decay between them on survey stations inside the grid survey area. The station plot point location is chosen as the midway point between the receiver (Rx) electrodes.*

The new GAIP survey data at Walbiri and at Dingo’s Rest were acquired using 50m spaced survey lines, 25m Rx dipole spacing, and 25m station spacing (Table 1), which are the same specifications as for the 2013 GAIP surveys. Tx electrodes were located approximately 500m outside of the survey block edge in a N-S direction for Walbiri, therefore highlighting primarily E-W trending IP anomaly responses and approximately an ENE-WNW direction for Dingo’s Rest, to highlight IP anomaly features oriented between NNW to N-S directions. The historical and recent GAIP survey areas are shown in Figure 2. For more information on the survey specifications, survey equipment and acquisition please refer to the survey reports by Zonge (Khrapov, 2013 and Mann, 2017).

***Table 1:*** *GAIP specifications for the Walbiri and Dingo's Rest GAIP surveys.*

| | 2013 | | 2017 | |
|---|---|---|---|---|
| | Walbiri | Dingo's Rest | Walbiri | Dingo's Rest |
| Survey line spacing (m) | 50 | 50 | 50 | 50 |
| Receiver dipole spacing (m) | 25 | 25 | 25 | 25 |
| Station spacing (m) | 25 | 25 | 25 | 25 |
| Tx electrode orientation (degree) | 0-180 (N-S) | 50-230 (NE-SW) | 0-180 (N-S) | 80-260 (ENE-WSW) |

ResPot imported the raw GAIP data into specialised software TQIPdB to review the primary electrical signal to noise levels, as well as the raw voltage decays for each reading to check for consistency and reliability during the survey period. The data were found to be of good quality and required little editing and cleaning. Preliminary processed GAIP grid data products and survey progress updates were provided to EME during the survey.

The final GAIP datasets were then imported into Oasis Montaj software where it was processed, filtered and gridded, and a suite of georeferenced ECW images and contour vector files were then generated using ER Mapper software. Figures 5 and 6 show examples of the GAIP chargeability, resistivity and conductivity results, respectively, for Dingo's Rest and Walbiri. The suite of images generated includes images of the standard chargeability, resistivity and conductivity data (inverse of resistivity), with varying sun angles and colour tables. In addition, a suite of half (0.5vd), and 1$^{st}$ vertical derivative (1vd) filtered images of each data type, and ternary red-green-blue (RGB) images of all three data types, were generated to highlight subtle IP anomalies and trends, and breaks in IP anomaly trends, which could be related to faults and other cross-structures.

ResPot went above the scope of work, at no extra cost, to obtain the historical GAIP survey data for Dingo's Rest and Walbiri, and carried out the same data processing and imaging as completed for the new survey data, so that a comparative set of images are provided for the old survey data for these two prospect areas.

All final GAIP data images have been provided in digital format as MapInfo registered ECW files accompanying this report. Contour vector files have also been generated for the IP data grids, and are provided in MapInfo TAB file format. Coordinates for all digital images and vector files are in datum GDA94 and projection MGA Zone 52.

### *2.1.2. GAIP Results and Observations*

At Dingo's Rest, the amplitude of GAIP chargeability anomaly values that were measured in 2013 and 2017 are very similar, and range from 0.9 msec to 8.5 msec. A NE-SW trending zone of subdued GAIP chargeability response near the centre of the new survey grid is likely due to a structural zone cross-cutting the stratigraphy, based on the magnetic response observed in airborne magnetic imagery previously generated by ResPot (Figure 5). The new Dingo's Rest GAIP survey assists tremendously in mapping resistive lithological units at prospect scale, particularly by using the 0.5VD and 1VD filters, and resistive units can potentially be tracked through the southern side to the north side of the interpreted cross-cutting structural zone near the centre of the grid. Relatively conductive IP responses observed in the new GAIP data are likely related to litho-dependant weathering in the regolith overlying resistive fresh bedrock.

At Walbiri, there is no indication that the reduced sandstone horizon, interpreted on the northern limb of the anticline, continues around the interpreted anticline fold axis and is present on the southern limb in the new GAIP survey grid. However, the GAIP survey coverage should ideally be extended to the north of the new survey grid to better resolve IP chargeability anomalism on its northern margin. A NE-SW oriented paleo-drainage, interpreted from airborne magnetic and radiometric data, is potentially masking the southern limb IP chargeability anomaly response. The strongest IP chargeability anomaly response on the northern margin of the new GAIP survey grid may actually be closer to the centre of the interpreted anticline, and so may indicate a complex structural zone or asymmetric folding, and even possibly that the southern limb is faulted along the fold axis.

CHARGEABILITY RESISTIVITY CONDUCTIVITY

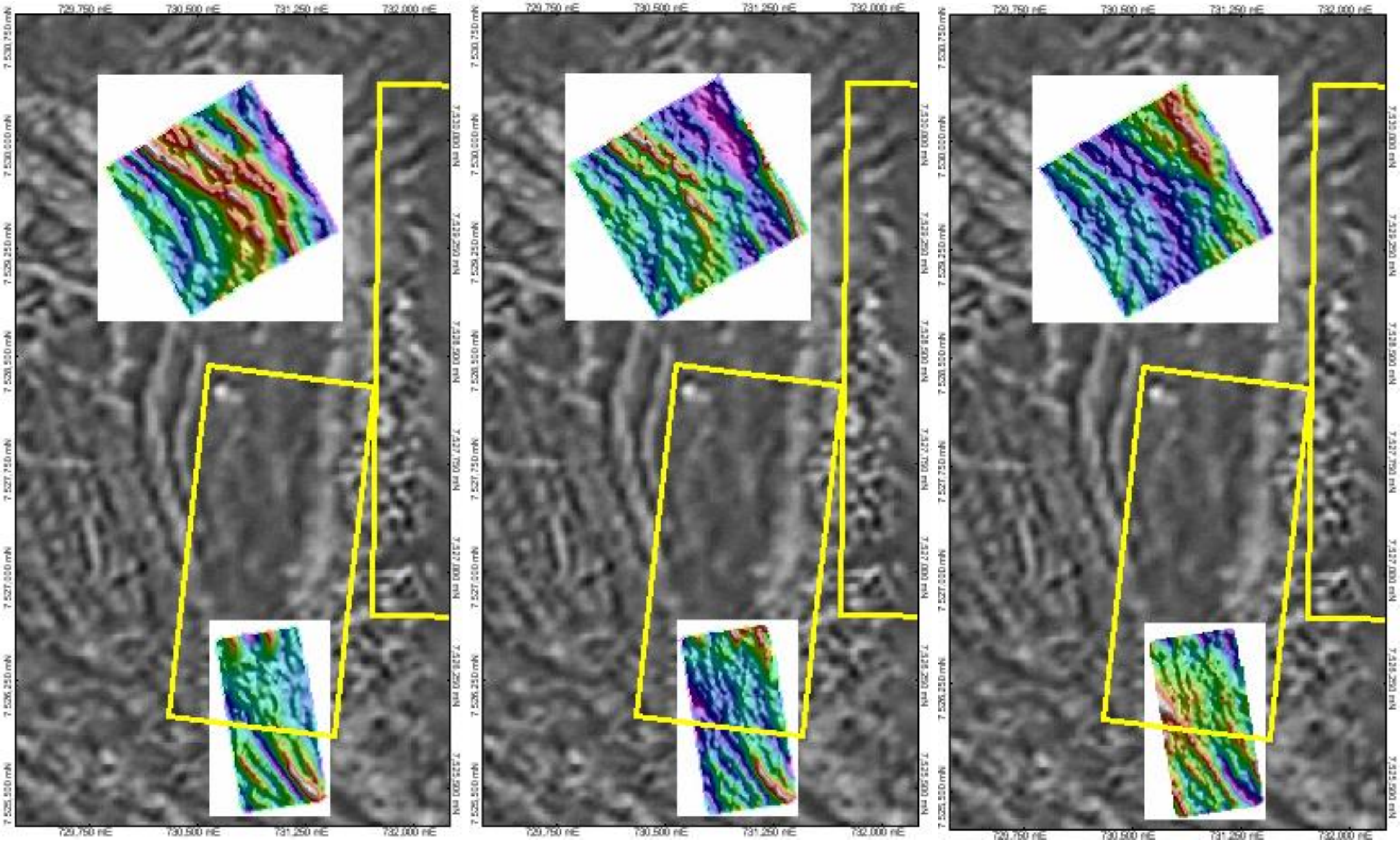


***Figure 5:*** *Final GAIP chargeability (left), resistivity (centre) and conductivity (right) images (all with NE sun shading) at Dingo's Rest, overlain on a magnetic TMIRTP-1VDAGC greyscale image with tenement outlines shown by the yellow lines. The 2017 GAIP survey data are located to the south from the 2013 GAIP survey data.*

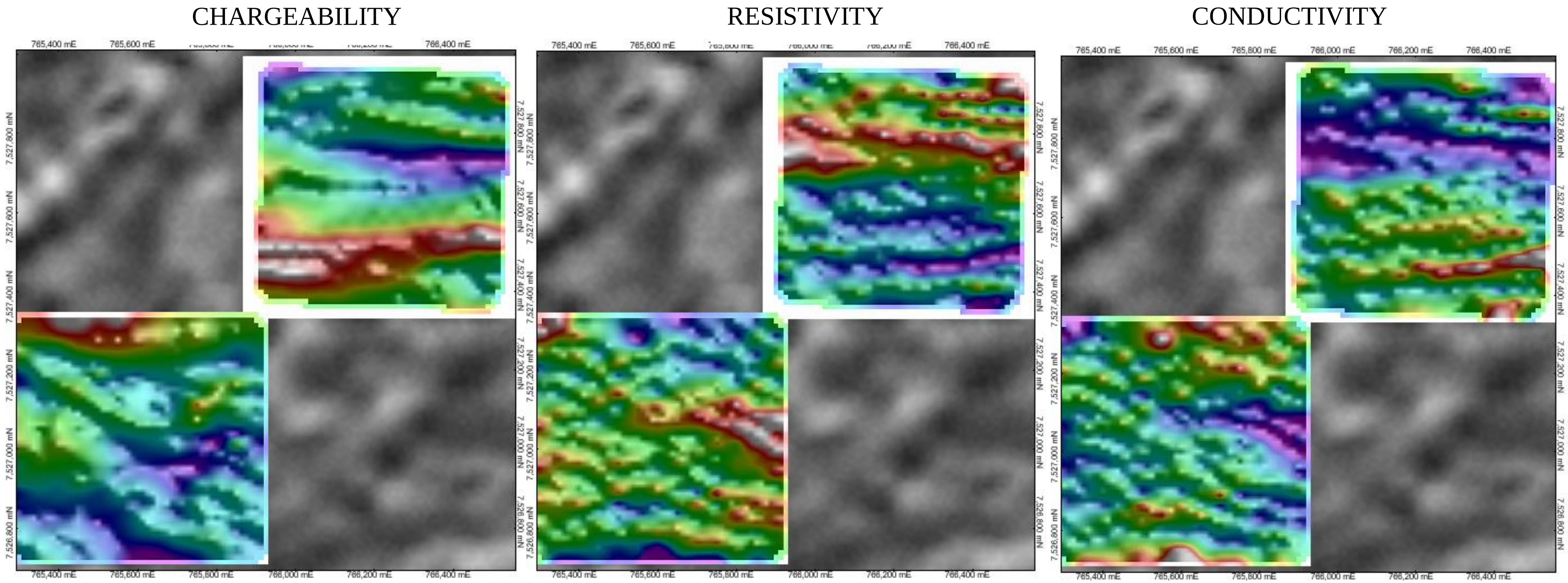


***Figure 6:*** *Final GAIP chargeability (left), resistivity (centre) and conductivity (right) images (all with NE sun shading) at Walbiri overlain on a magnetic TMIRTP-1VDAGC greyscale image. The 2017 GAIP survey data are located to the southwest from the 2013 GAIP survey data.*

## 2.2. Pole Dipole IP (PDIP)

### *2.2.1. Survey specifications and processing*

PDIP surveys employ a local single pole Tx electrode and dipole Rx pair, which are separated by some distance along the survey line and moved around to obtain IP information at greater depth than GAIP surveying. The distance between the Tx and Rx pair is related to the depth of investigation, so as the distance between the Tx and Rx separation is increased, increasing N-levels, then the data observation point will be deeper. Raw PDIP data are presented as pseudosections, where the data observation point is presented as the midway point between the Tx and Rx electrode pairs, defined by the intersection of angled lines extending down from the centre of the Tx and Rx electrodes (Figure 7).

Figure 7 shows a schematically representation of a PDIP pseudosection and the pseudo depths as N-levels.

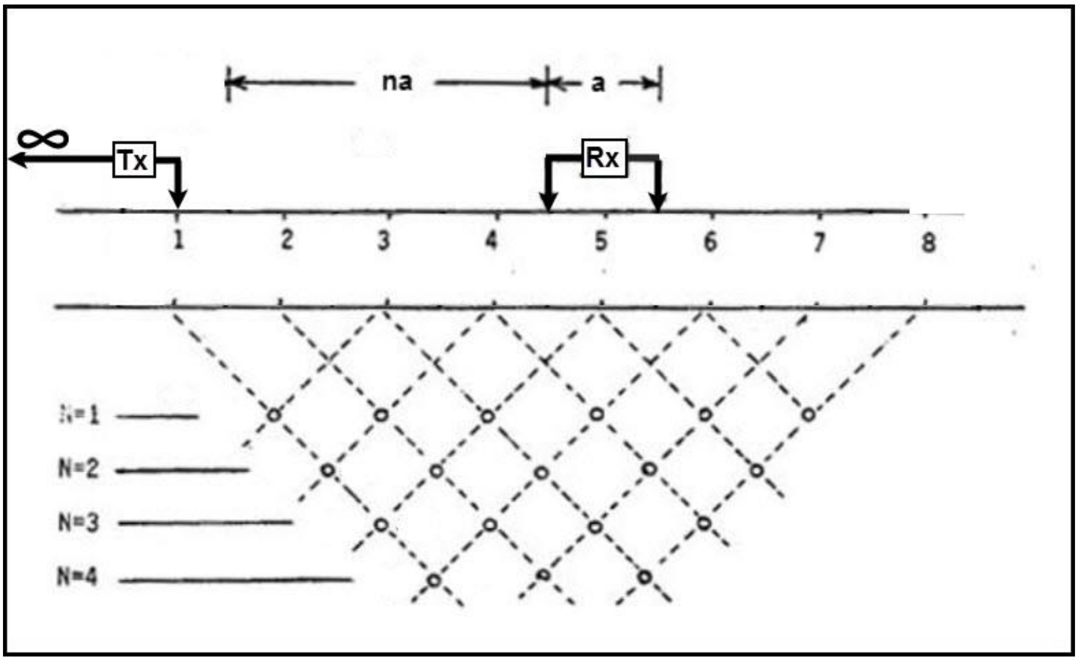


***Figure 7:*** *Schematic representation of how PDIP pseudosections are generated. The data observation point is the midway between the Tx and the Rx electrode pair, defined by the intersection of right angled lines.*

The regional location of the Yuendumu West PDIP survey line is shown in Figure 2. The PDIP data were acquired by Zonge along 1.7 km long survey lines, using 50m receiver dipole spacing and 50m station spacing, recording with 24 channels (N=24). Initially, a dipole-dipole IP (DDIP) array was trialled for the Yuendumu West survey line. However, inadequate signal current and anomaly levels were recorded at depth (deeper N-levels), so the survey was carried out using the PDIP array, which has greater depth penetration but less near surface resolution than DDIP. ResPot liaised with Zonge to review the initial DDIP data, and then make a change to employ the PDIP configuration. PDIP surveys increase signal at depth but also lose little bit of a loss of resolution in the near surface compared to DDIP surveys. PDIP surveys also result in angled anomaly zones in raw data pseudosections for steeply dipping features, which is quite different to the classic "pants leg" and triangular anomaly shapes that are observed for steeply dipping features in DDIP pseudosection data.

ResPot's data QC and editing process involved importing final raw PDIP data into a TQIPdB database and reviewing the IP decays at each data point along each line to determine the data quality. Several poor data points at deeper N-levels were identified and removed (Figure 8).

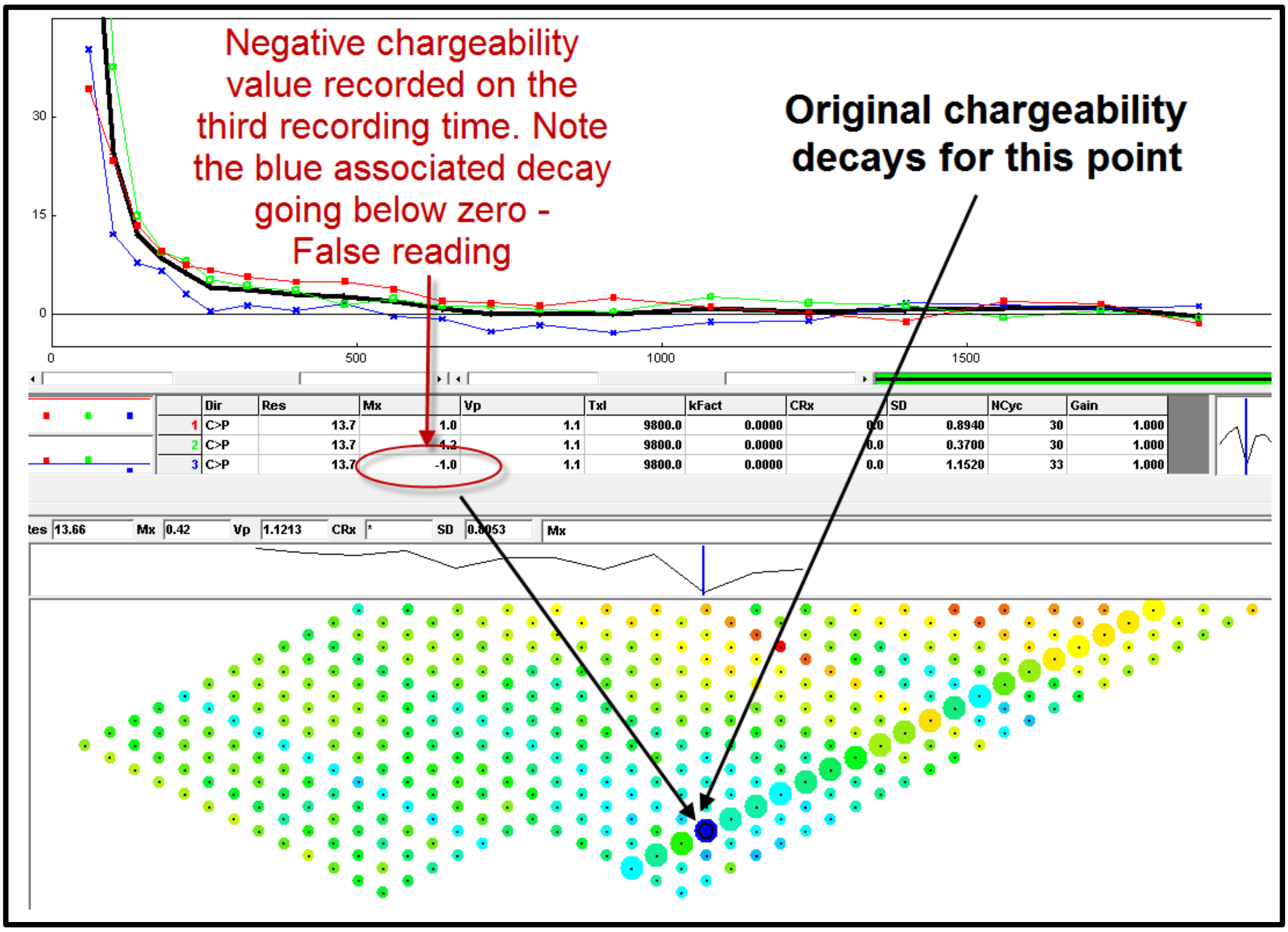


***Figure 8.*** *Example of PDIP data editing along the Yuendumu West PDIP survey line using TQIPdB software. The three IP decays (top panel) correspond to three readings taken for the data point highlighted in the bottom panel. The third reading (blue) displays a calculated negative chargeability value and a noisy decay curve, hence have been removed prior to inversion modelling.*

PDIP inversion processing was carried out on the edited PDIP data using the University of British Columbia inversion code DCIP2D. This is a smooth-model inversion code which is an industry standard for inverting PDIP data. The inversion model process converts the raw observed resistivity and chargeability data pseudosections into Earth model cross sections of the data.

Plots of the ResPot PDIP inversion results are shown in Figure 9. For each IP data type (resistivity and chargeability), the pseudosection plots show the observed and plotted pseudosection (upper panel), modelled pseudosection based on the inversion result (centre panel), and final inversion model as a depth cross section (lower panel). The inverted model pseudosection is the final result of inversion processing and represents the Earth model pseudosection for comparison to the observed pseudosection. The modelled pseudosection is used to check the accuracy and reliability of the inversion processing, where a good match between the modelled data and observed data indicates a better inversion model.

Note that while ResPot have completed some data editing, some small and very low amplitude data errors are still present in the edited raw chargeability data at deeper N-levels. However, they have not been modelled by the inversion process and so they are not adversely affecting the inversion model results (Figure 9).

ResPot have clipped/masked the inversion model section to remove padding at the edges, and is based on the spatial coverage of the observed data acquired at depth, and therefore the sections have angled sides. This is carried out to avoid displaying false anomalies within the padding area of the inversion model.

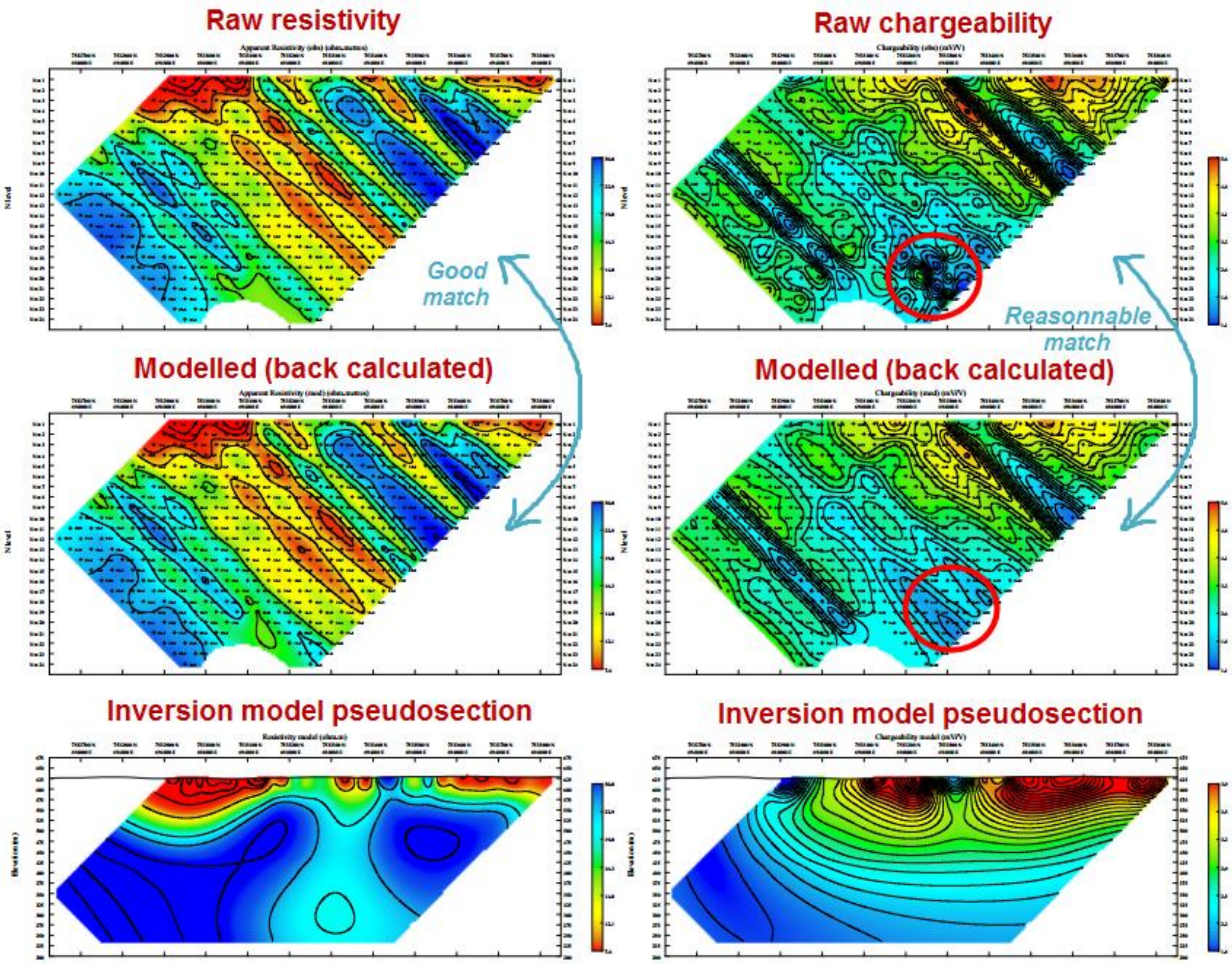


***Figure 9.*** *PDIP resistivity (left) and chargeability (right) inversion processing results for the Yuendumu West PDIP survey line 694000E. Note that the resistivity data sections are coloured such that "hot" colours represent higher conductivity. The red circle on the raw and modelled chargeability pseudosections shows where some small data errors/noise is present in the raw data, bit not modelled by the inversion process, and therefore not having an adverse effect on the inversion result.*

Zonge also processed and inverted the PDIP chargeability and resistivity data, and these inversion results can be found in their acquisition and processing report (Mann, 2017).

The ResPot inversion processing results were compared to the Zonge inversion results, and both are deemed to be similar. However, the Zonge inversions may be preferred because they enhance vertical IP anomaly features, which may be due to structures and/or contacts. Figures 10 and 11 compare the IP resistivity and chargeability inversion models generated by Zonge and ResPot. For the resistivity data, both Zonge and ResPot inversion model sections are coloured such that red is more conductive; note that the Zonge inversions were not clipped to the survey coverage, and therefore false information is displayed in the padded areas at the sides of the models.

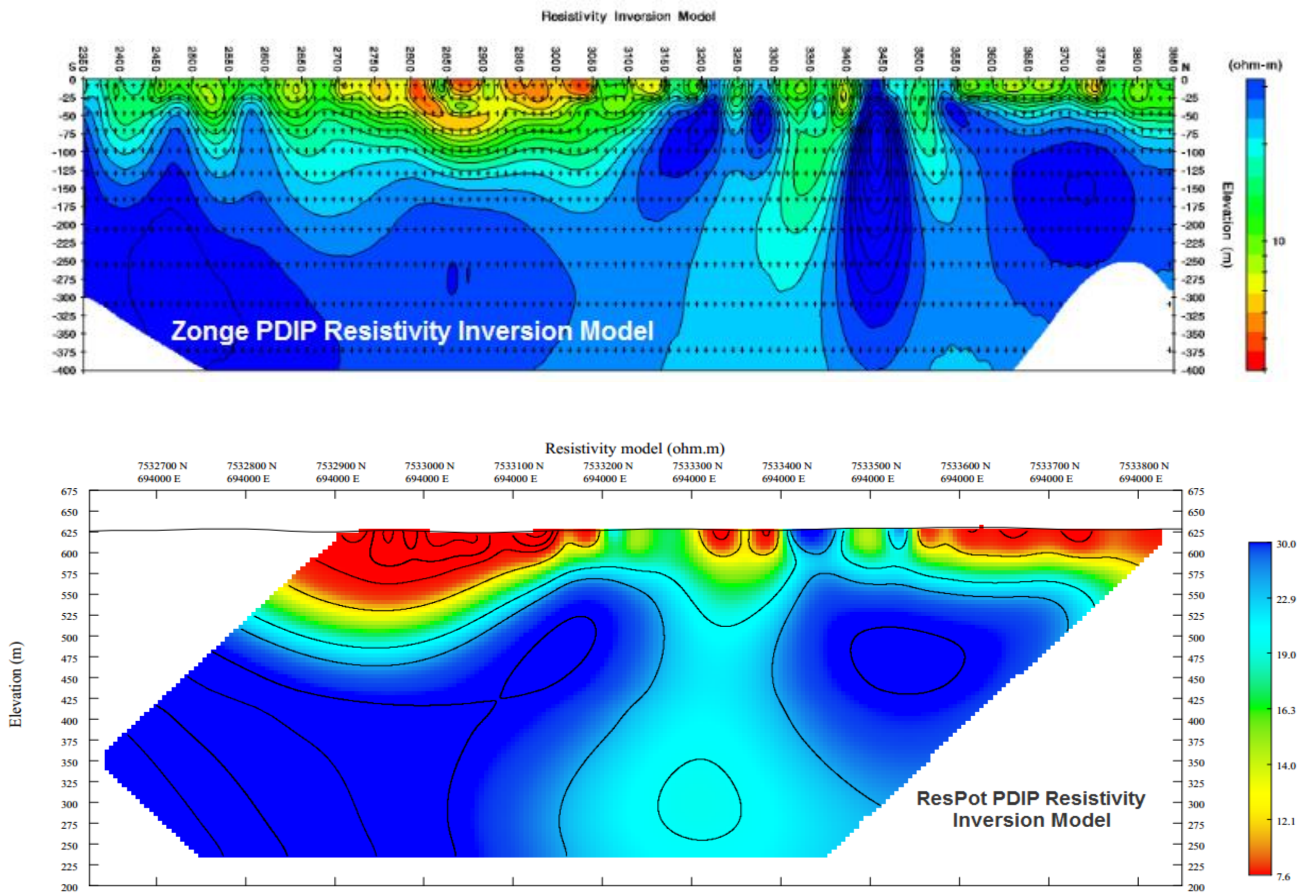


***Figure 10****: Comparison of the Zonge (top) and ResPot (bottom) resistivity inversion model sections for the Yuendumu West PDIP survey line 694000E. Relatively resistive zones are in blue and conductive zones are red. Note that the sections use a different horizontal axis, where the Zonge inversion model section is shown in local survey grid parameters and the ResPot inversion section is shown in projected coordinates (GDA94/MGA Zone 52).*

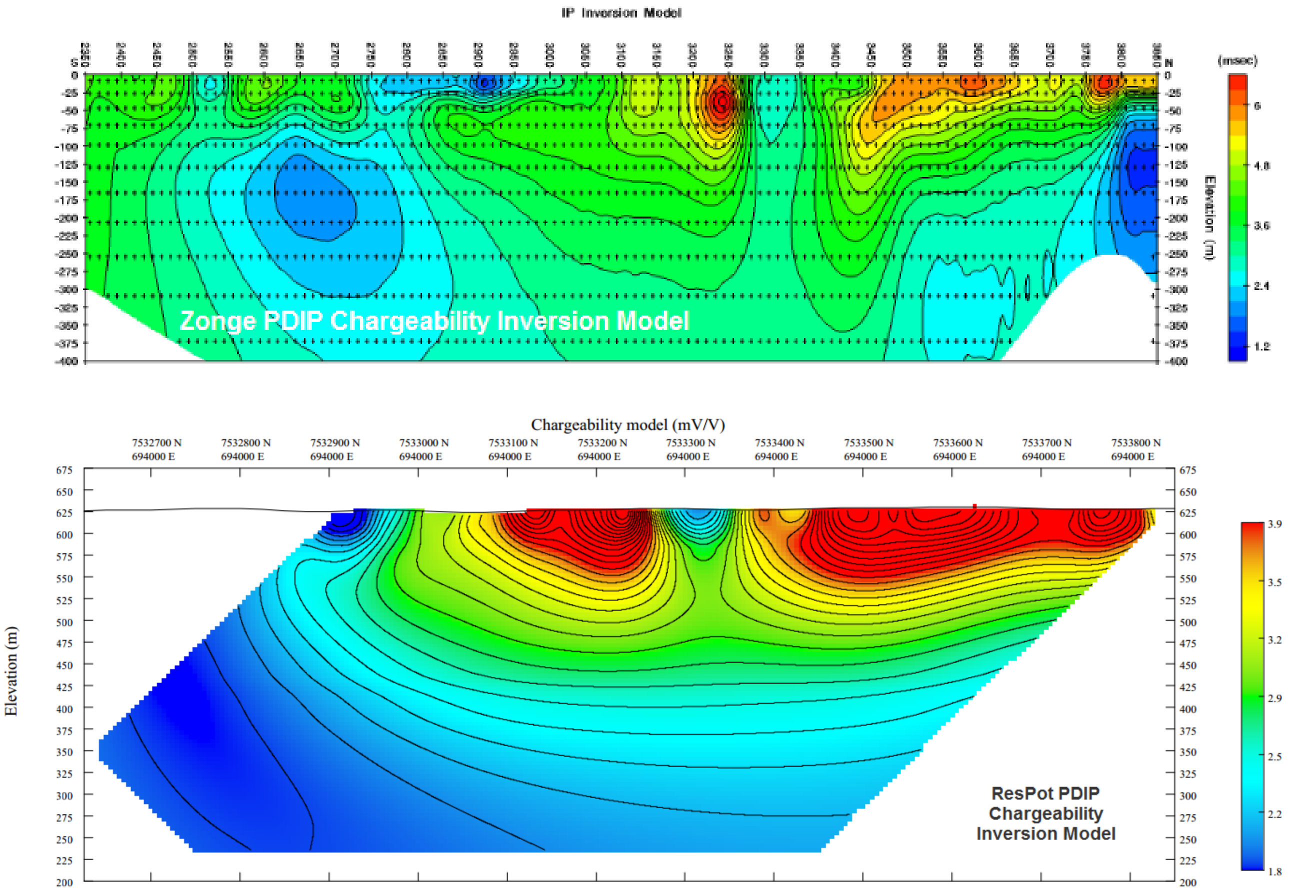


***Figure 11:*** *Comparison of the Zonge (top) and ResPot (bottom) chargeability inversion model sections for the Yuendumu West PDIP survey line 694000E. Note that the sections use a different horizontal axis, where the Zonge inversion model section is shown in local survey grid parameters and the ResPot inversion model section is shown in projected coordinates (GDA94/MGA Zone 52).*

### *2.2.2. PDIP Results and Observations*

Based on EME interpretation of airborne magnetic images, the Yuendumu thrust is expected to occur at approximately 7533200N-7533270N along the PDIP survey line. A vertically shaped resistivity PDIP inversion model low anomaly in this position is likely caused by the Yuendumu thrust, and potential back thrusts located to the south of Yuendumu thrust, which is consistent with the magnetic data, but also with the broad conductive response in the ResPot PDIP resistivity inversion model section (Figure 10). Note the conductive regolith cover has variable thickness in the inversion model.

Note that there are multiple angled resistivity low anomalies in the raw PDIP data pseudosection, which is characteristic of multiple steeply dipping sources (likely either structure or lithological contacts), but these are poorly represented in the inversion model section. This is typical of inversion modelling, which is unable to account for all of the detailed anomaly variations in the raw data, and only produces large broad inversion model anomalies; even for discrete and thin sources. Therefore, interpretation of the PDIP pseudosections is important for getting more detailed anomaly information.

The PDIP chargeability inversion model anomalies are mostly confined to the near surface, and most likely represent polarisable clays in the weathering profile, which extend below the regolith layer in the resistivity inversions and may in turn vary depending on structure and lithology.

## 3. Conclusions and Recommendations

This report provides a summary of the IP surveying work carried out at the Ngalia Basin Project in 2017, and describes the data processing, imaging and modelling of the IP survey data carried out by ResPot. Some basic observations of the IP results and simple integration with previous airborne magnetic survey results are presented, but detailed interpretation, targetting and drill planning was not part of the work scope.

During this work, ResPot have also obtained a lot of project data from EME, and have spent un-billed time to sort through the GIS datasets, and integrate relevant datasets into GIS workspaces. It is recommended that a second stage of interpretation and targetting of the geophysical data be carried between EME and ResPot staff out to provide more insight into potential uranium mineralisation prospectivity and targets, and assist with planning drillholes. In particular, it is recommended to complete detailed interpretations of key prospect areas by creating A0 size plots at appropriate scales and carrying out an interpretation of bedrock lithology and structure in each prospect area. The airborne survey magnetic, radiometric and DTM data previously acquired would be key datasets in these interpretations. The interpretation work would then be digitised to create GIS vector files to provide a useful reference layer for future exploration work and targetting.

# 4. References

Kerr, S. and Taylor, W., 2015, Part 1: Walbiri and Walbiri South Prospects, Ngalia Project Prospectivity Analysis, Ngalia Basin, NT – part 1 of 4. Energy Metals Technical Memorandum, 27p.

Khrapov, A., 2013, Bigrlyi Gradient Array Induced Polarisation Survey. ZONGE report No 130058, 35p.

Mann, S., 2017, Ngalia Gradient Array and Pole-dipole Induced Polarisation Survey. ZONGE report No 170308, 17p.

Owers, M., 2015, Ngalia Basin high-resolution magnetic survey planning, QC, processing and imaging. Resource Potentials summary report. 17p.

Xiao, S., Kerr, S., and Taylor, W., 2015, Part 4: Dingo's Rest – Carnotite Hill Corridor, Ngalia Project Prospectivity Analysis, Ngalia Basin, NT – part 4 of 4. Energy Metals Technical Memorandum, 25p.